JOURNAL OF MAGNETIC RESONANCE **130,** 1–7 (1998)
ARTICLE NO. MN971282

Analysis of Polymer Materials by Surface NMR via the MOUSE

A. Guthausen, G. Zimmer, P. Blümler, and B. Blümich

Lehrstuhl für Makromolekulare Chemie, Worringer Weg 1, 52074 Aachen, Germany

Received April 28, 1997; revised September 23, 1997

Applications are discussed of a novel NMR device, the NMR MOUSE (*mo*bile *u*niversal *s*urface *e*xplorer), for characterization of polymers. Different properties of elastomers can be related to an effective transverse relaxation parameter $T_{2\text{eff}}$. Effects of multiecho sequences influence the decay curve and can be described in terms of B_0 inhomogeneity and spin-lock effects. Furthermore, the signal-to-noise ratio (S/N) can be improved by use of steady-state free precession (SSFP) pulse sequences modified for use in inhomogeneous magnetic fields. © 1998 Academic Press

Key Words: **polymers; surface NMR; NMR MOUSE; inhomogeneous fields; nondestructive testing.**

INTRODUCTION

NMR has been shown to be a powerful method for the investigation of elastomers (*1*). Relaxation parameters, as for example T_2 and $T_{1\rho}$, are sensitive to fluctuations in a frequency range of a few kilohertz, which is typical for slow molecular motions. This is also the frequency range where molecular motion is directly related to the mechanical properties of elastomer materials (*2*). In ^{1}H NMR, the most important interaction, which is modulated by molecular motion, is the dipolar coupling. It has been shown that, for example, differences in cross-link density, temperature, pressure, strain, and aging processes can be monitored by T_2 and $T_{1\rho}$ (*3*). These relaxation times are also used as contrast parameters in NMR imaging of elastomers (*1*).

The sensitivity of relaxation parameters to material properties allows a modified approach with respect to NMR imaging: The intrinsic relaxation parameters depend on magnetic field strength, but not on the homogeneity of B_0 and B_1 within certain limits. Instead of using the highly homogeneous magnetic fields as in conventional NMR spectroscopy one can perform relaxation measurements in inhomogeneous fields, which can easily be realized by one-sided permanent magnets and surface coils. Such an NMR device is the NMR MOUSE (*4*). In contrast to conventional NMR where the probe supplies only the RF magnetic field B_1, the MOUSE probe consists of two permanent magnets with anti-parallel magnetization, producing the B_0 field parallel to its surface. For B_1 irradiation, a surface coil is mounted in between the magnets which generates a magnetic field perpendicular to the surface. A similar approach can be found in (*5*). The advantage of this concept is that restrictions of the sample geometry no longer exist. However, the sensitive volume is restricted to regions near to the surface of the object under examination. It depends on the B_0 and B_1 distribution and is therefore determined by the geometry of the B_1 coil and of the permanent magnets. The design of the probe can be adjusted to different applications. For the measurements presented here we used a carrier frequency of 17.5 MHz and a coil geometry, which selects a volume of about 9×4 mm in plane and 0.5 mm in depth. Further details are published in (*4*).

NMR RELAXATION PROBED BY INHOMOGENEOUS FIELDS

The given inhomogeneities of B_0 and B_1 require reexamination of well-known pulse sequences and development of new pulse sequences. The aims are an improved understanding of the origin of the measured signal, a reduction of measuring time for efficient *in situ* measurements, and an optimization of the signal sensitivity toward changes in material properties. Because of the importance of the dipolar couplings for characterization of elastomer properties, Hahn echo, solid echo, and their multiecho versions (CPMG (*6*) and OW4 (*7*), respectively) were applied to samples with nominally different cross-link densities. The difference between the pulse sequences is the refocusing of interactions bilinear in spin operator I, for example, of homonuclear dipolar interactions, by a $\pi/2$ pulse, while a π pulse refocuses only magnetization dephasing from interactions which are linear in I, for example, chemical shift and field inhomogeneity effects.

Results of the corresponding multiecho sequences are shown in Fig. 1, where the dependence of the effective relaxation time on the pulse length is examined. In contrast to conventional NMR, the flip angle depends on spatial coordinates due to the field inhomogeneity for a given pulse length. A defined flip angle therefore exists only within a sufficiently small volume element. Thus we define the pulse length resulting in zero signal as π pulse, and when obtaining maximum signal the pulse length is referred to as a $\pi/2$ pulse. The echo sequences can be described as $\theta_x-(\tau-2\theta_y-\tau)_n$

1090-7807/98 $25.00

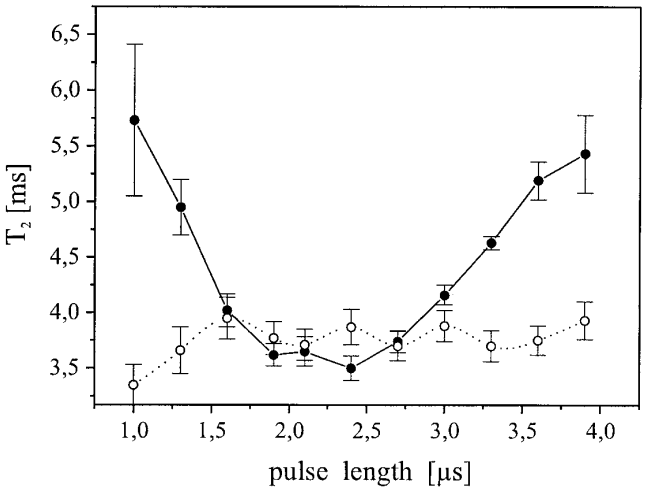

FIG. 1. Effective T_2 relaxation times of an unfilled SBR sample obtained from measurement of multiecho trains as a function of pulse length. (○) Only the preparation pulse (nominal $\pi/2$ pulse) is varied. The dependence of T_2 on the flip angle (expressed by pulse length) is quite weak. (●) Relaxation times obtained by varying both preparation and refocusing pulses. A strong dependence on the nominal flip angle is observed. The minimum of T_2 corresponds to the best approximation to a $\pi/2-\tau-\pi$ echo sequence ($\pi/2 = 2.25\ \mu s$).

and $\theta_x-(\tau-\theta_y-\tau)_n$ for multiple Hahn and solid echoes, respectively. Two experiments were performed: The open circles represent relaxation times obtained by varying only the angle θ of the excitation pulse, which is expressed by the pulse length. The refocusing pulse 2θ was adjusted to a value near π, which amounts to about 4.5 μs. Within the experimental error, almost no flip angle dependence is observed. However, changing both pulse lengths simultaneously reveals a strong dependence of the effective T_2 relaxation parameter on the flip angle which can be assigned to the different properties of the refocusing pulse by comparison of the two measurements.

Because of the inhomogeneous B_1 field an intrinsic flip angle distribution must be considered in addition to the induced variation of the pulse length in the experiment. As a consequence, partial averaging of the dipolar interaction is spatially dependent. Figure 1 shows that a strong dependence of the echo-decay time on the pulse length of the second pulse exists. The question arises whether the flip angle dependence is due to an averaging of the dipolar interaction or due to imperfections of the experiment, for example, changes in the sensitive volume. Different authors have shown that in the case of much less inhomogeneous fields an intrinsic flip angle dependence of the relaxation parameter in a multiecho sequence exists (*8–10*). Even more, phase glitches and field inhomogeneities leading to highly imperfect pulses do not allow for a physically accurate determination of the relaxation parameter T_2 a priori. However, monitoring differences in material properties does not require the exact measurement of the microscopic relaxation rate, as long as a functional relationship between the mechanical properties of an elastomer and the measured effective T_2 value can be established. In addition, industrial samples can show large inhomogeneities below the spatial resolution limit of NMR. Therefore, experimentally determined NMR relaxation times can be spatial averages, which are defined by the experimental setup, and do not necessarily represent relaxation times for microscopically homogeneous volume elements.

Figure 1 shows that the intrinsic distribution of relaxation times due to the B_1 inhomogeneity is smaller than that induced by pulse angle variation on the spectrometer. This result demonstrates that despite inhomogeneous B_0 and B_1 fields relaxation measurements are relatively well defined. The dependence of the effective T_2 on the flip angle can therefore be explained by the partial averaging of the dipolar coupling by the refocusing pulses and consequently allows the discrimination of different interactions like chemical shift and field inhomogeneity on one side and dipolar coupling on the other.

In addition to the influence of dipolar coupling on the echo decay, an effect of the inhomogeneous magnetic fields can be observed. In Fig. 2, the amplitudes of the first few echoes are shown, normalized to the amplitude of the first echo. Instead of an intensity *decrease* due to T_2 relaxation, first an *increase* is found which strongly depends on the flip angle and on the echo time (not shown here). The shorter the flip angle, the more pronounced is the increase of the echo amplitude. Also the maximum intensity occurs at different echo numbers, but is nearly independent of the echo time. This observation is rather unusual from the point of

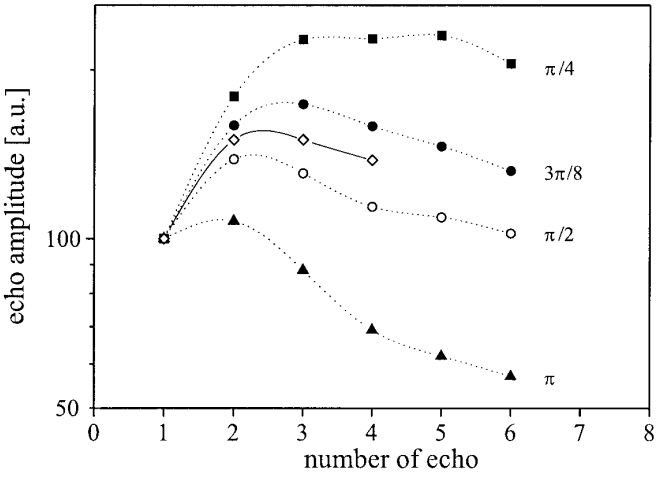

FIG. 2. The initial increase of the echo amplitudes (normalized to the amplitude of the first echo) strongly depends on the flip angle. A comparison of these data with calculations of the OW4 sequence for STRAFI conditions (solid line) shows good agreement and leads to the conclusion that the effect is mainly due to the B_0 inhomogeneity, i.e., the magnetic field gradient.

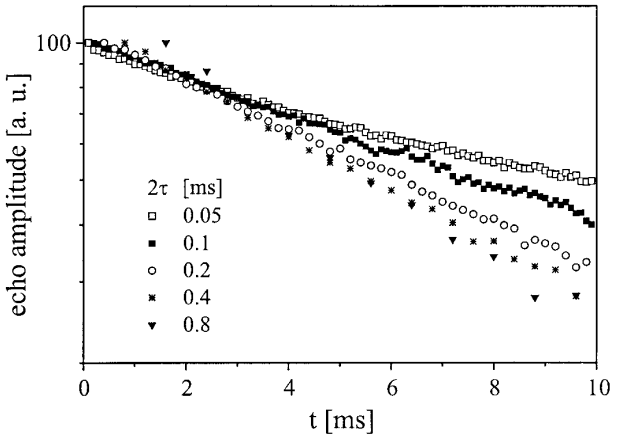

FIG. 3. Apparent spin-lock effect in a CPMG experiment. The different slopes of the decays reflect the different effective spin-lock fields produced by a variation of the echo time 2τ.

view of conventional NMR. However, we are dealing with highly inhomogeneous B_0 and B_1 fields, leading to a distribution of flip angles as well as of effective fields. The reason for these findings is the evolution of the magnetization under the influence of the field gradient leading to strong spatial modulation and interference of echo signals from different voxels. It should be noted that the sensitive volume changes as a function of pulse length as well as the degree of mixing of longitudinal and transverse magnetization which is the reason for different modulation patterns of the transverse magnetization. This behavior is also found in stray-field imaging (STRAFI) experiments as far as B_0 inhomogeneities are concerned and was calculated for the OW4 sequence by solving the Bloch equations for this particular case (*11*). The rotation of the magnetization vector is calculated in the rotating frame, taking into account the spatial dependence of the effective field. A comparison with the results by the NMR MOUSE shows quite good agreement in the case of the OW4 sequence (Fig. 2). This agreement leads to the conclusion that the B_0 inhomogeneity is the main reason for the initial increase of the echo amplitude. It is interesting to note that a similar behavior is found despite the fact that about constant B_0 gradients are involved in STRAFI experiments and nearly linear B_0 gradients for the MOUSE.

Apart from the influence of B_0 inhomogeneity an effect comparable to the spin-lock effect in homogeneous fields is observed. It can easily be demonstrated by varying the pulse distance τ, which is shown in Fig. 3 for the CPMG sequence (nominal $\theta_x-(\tau-2\theta_y-\tau)_n$). The sample used in this experiment was an unfilled, cross-linked styrene butadiene rubber (SBR) with a content of 0.75 phr DICUP (dicumylperoxide on caolin; phr, parts per hundred rubber). Note the τ dependence of the slope in the semi-logarithmic plot. This effect can be observed in the case of the OW4 sequence as well as in the case of CPMG pulse trains. The dependence of the effective relaxation times on the pulse distance τ bears similarity to the magnetization behavior in an effective spin-lock field as observed in classical NMR. Preliminary experiments using conventional spin-lock sequences support this interpretation. Spin-lock effects can in principle be avoided by using phase alternating multiecho sequences as, for example, MLEV-*n* (*12*). The main feature of these pulse sequences is the fact that the phase difference between refocusing pulses always amounts to 180°. This leads to different dephasing behavior of M_x and M_y magnetization components. Strong modulation of the echoes occurs, which gives rise to rapid signal loss and consequently low sensitivity as also observed in STRAFI experiments (*11*).

As shown for example in (*10*), this behavior can in principle be avoided by applying a series of pulses with 90° phase shifts (for example, XY-16 sequence: refocusing pulses *xyxy yxyx* $-x-y-x-y$ $-y-x-y-x$), resulting in decay times comparable to those obtained by a CPMG sequence in homogeneous fields. Results of CPMG and XY-16 measurements by the NMR MOUSE are shown in Fig. 4. In this experiment, an SBR with a content of 1.25 phr DICUP was used. Relaxation times deduced from magnetization decays are compared for CPMG and XY-16 echo trains. Obviously, the inhomogeneities of B_0 and B_1 lead to flip angle variation and influence the time constants at short echo times 2τ. At longer echo times, the spin-lock effect is less efficient (CPMG) as the effective lock field is reduced. The relaxation times approach those obtained by XY-16 for long echo times. Note the independence of the effective T_2 for a wide range of τ values for the XY-16 sequence. By comparison with the CPMG results for a

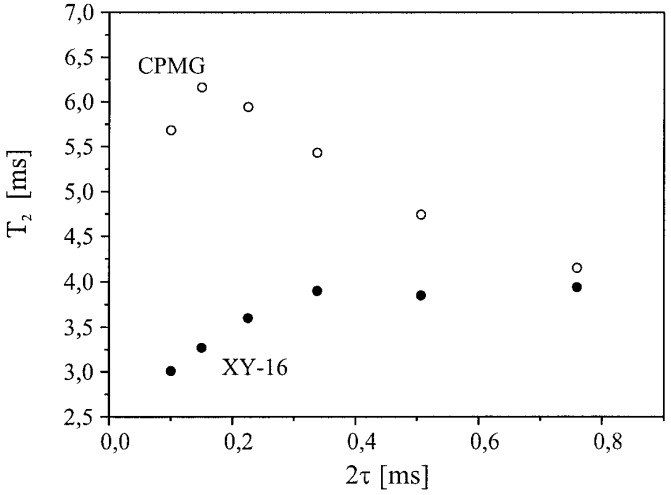

FIG. 4. Effective relaxation times T_2 as obtained from CPMG and XY-16 sequences. At short echo times 2τ, the differences between the two pulse sequences are obvious: Due to the pulse phases used in a CPMG sequence, a spin-lock effect can be observed. For measuring T_2, the XY-16 sequence can be used at reasonable echo times. Note the convergence of the relaxation times at long echo times.

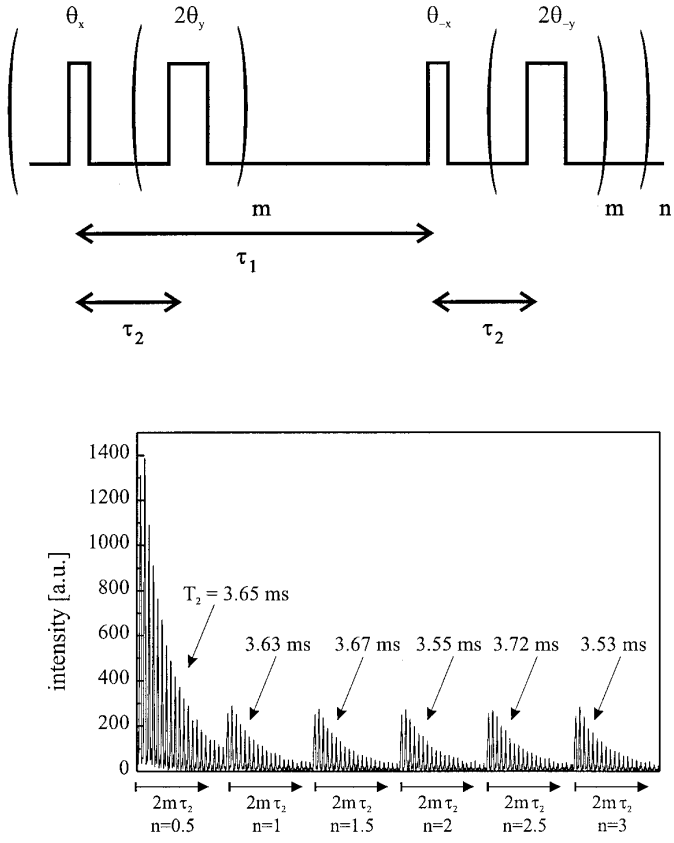

FIG. 5. SSFP–CPMG pulse sequence and observed echo trains. The first echo train starts from Boltzmann equilibrium (BE), whereas the following echo trains show the amount of SSFP magnetization. A monoexponential fit to the data reveals no systematic deviation of T_2 when starting from the dynamic equilibrium (DE).

given effective spin-lock field, the spin–lattice relaxation time $T_{1\rho}$ in the rotating frame can be estimated.

SIGNAL-TO-NOISE IMPROVEMENT

Because of the low magnetic field strength and the use of surface coils the S/N ratio of the NMR MOUSE is low compared to conventional NMR in high magnetic fields, but envisioned industrial and medical applications of the method require short measurement times. In order to improve the S/N ratio steady-state magnetization can be used (*13, 14*). Here, phase-alternated pulses are applied with a fixed delay shorter than $5T_1$. Consequently, a dynamic equilibrium is established between excitation and relaxation. Depending on flip angle and delay, different amounts of transverse and longitudinal magnetization can be generated, which allows the reduction of measurement time like the use of the Ernst angle in high-resolution NMR (*14*). Because of the strong magnetic field gradient of the MOUSE the FID, which is usually detected in such steady-state free precession (SSFP) experiments, is too short to be observed. Instead of using only phase alternating θ pulses to induce an SSFP signal (*13*), refocusing pulses were added to generate echoes, which can easily be detected. Depending on the repetition time τ_1 of the SSFP pulses, longitudinal as well as transverse interferences can be observed. When τ_1 is reduced from about $5T_1$ (Boltzmann equilibrium (BE)) to values on the order of T_1 (dynamic equilibrium (DE)), the S/N ratio can be improved by a factor of about 2.5. For shorter τ_1 the improvement is even more pronounced by exploiting transverse interferences (factor 3 at least).

The SSFP magnetization can also be used to acquire CPMG echo trains. An example is given in Fig. 5 with the pulse sequence (top) and the experimental data from an unfilled cross-linked SBR sample (0.75 phr DICUP). While the first echo decay starts from BE, the amplitudes of the following echo trains are determined by the amount of SSFP magnetization. Here, the decay times do not depend on whether starting from BE or DE within experimental error. Thus, the decays can be coadded for S/N improvement. However, if T_1 differences arise within the sensitive volume or between different samples, CPMG (starting from BE) and SSFP–CPMG decays are no longer equivalent. This additional weighting can enhance the contrast between samples.

A further example of using the SSFP magnetization is the rapid measurement of T_1 and T_2 in one experiment (Fig. 6). In principle, T_1 is measured analogous to saturation recovery:

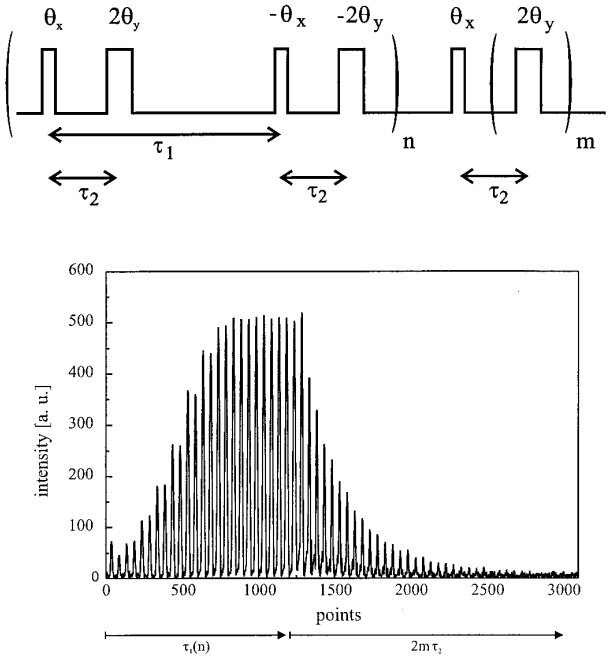

FIG. 6. Rapid determination of the two relaxation parameters T_1 and T_2. (Top) Pulse sequence. τ_1 is incremented in loop n for the measurement of T_1, whereas the T_2 relaxation is measured via a CPMG echo train (loop m). (Bottom) Experimental demonstration. T_1 relaxation is measured via steady-state magnetization from points 0 to 1249, which is proved by the acquisition of two consecutive echoes for each τ_1. The CPMG echo decay is displayed in the following points 1250 to 3000.

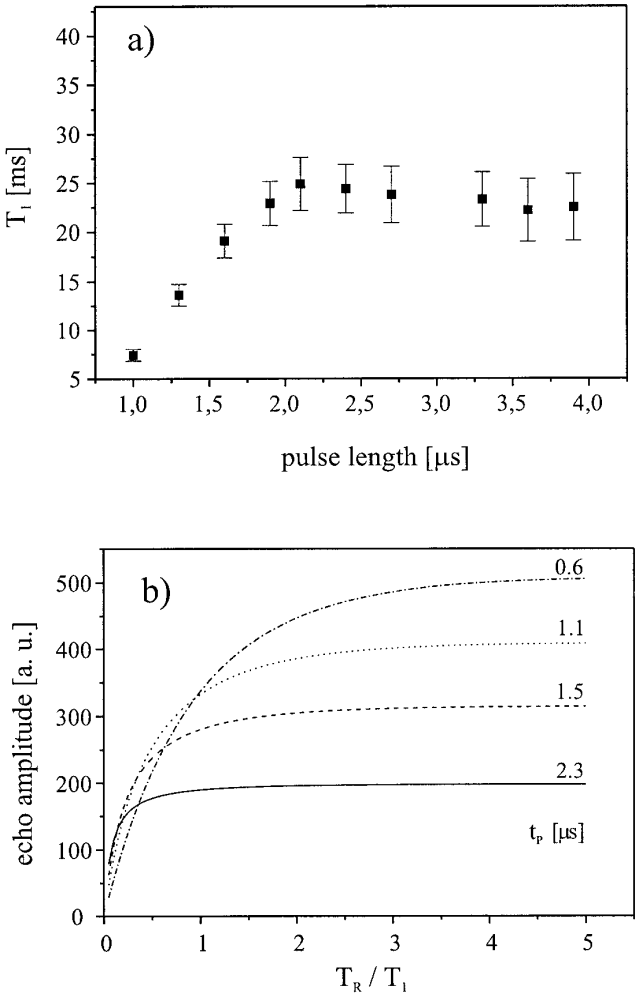

FIG. 7. Pulse length dependence of the effective longitudinal relaxation time. (a) Experimental recovery times as a function of pulse length (pulse sequence in Fig. 6). A pulse length of about 1.8 μs corresponds to a $\pi/2$ flip angle as deduced from maximum intensity of the signal. (b) Recovery curves for different pulse lengths. They depend on the ratio of repetition to longitudinal relaxation rate under steady-state conditions and were calculated by Eq. [1]. The deduced time constants clearly depend on the flip angle.

Depending on the delay τ_1 (Fig. 6 top), the magnetization recovery is measured. Ensuring that DE is established, about six dummy scans are included and also two following echoes are digitized for each τ_1 (points 0–1249). The recovery curve can be analyzed in terms of a usual saturation recovery which was proved by direct comparison of the two experiments. Subsequently T_2 is measured by a multiecho sequence (points 1250–2999).

Because of the inhomogeneity of B_1 an intrinsic flip angle distribution may influence the recovery of magnetization. As an intrinsic flip angle distribution can hardly be examined, the pulse length is varied to study its effect. The influence of pulse length on the recovery curve is quite pronounced (Fig. 7): For small flip angles, a reduction of the decay time is found, while the decay curve can still be described by $M(t) = M_0(1 - \exp(-t/T_1))$, where M_0 is the Boltzmann equilibrium magnetization. These findings are also observed in the case of SSFP NMR experiments in homogeneous fields and are described for example in (*14*). The observable SSFP magnetization $M_x(0^+)$ depends on the flip angle β as well as on the ratio of the repetition time T_R and the relaxation time T_1:

$$M_x(0^+) = M_0(1 - \exp(-T_R/T_1)) \times (1 - \exp(T_R/T_1)\cos\beta)^{-1}\sin\beta. \quad [1]$$

The SSFP magnetization described by Eq. [1] is shown in Fig. 7b as function of T_R/T_1 for different pulse lengths. The time constants which can be deduced from the simulated recovery curves show the same general behavior as the experimental data. Therefore, we conclude that for measurement of the T_1 relaxation it is necessary to adjust the pulse length to a plateau value.

APPLICATIONS

The methods discussed in the previous sections have been applied for measurements of industrial samples by the NMR MOUSE. As stated above, the effective relaxation time T_2 reveals differences in the cross-link density, strain, and temperature of elastomers (*1–3*). In order to verify the results by the NMR MOUSE, measurements were performed on the same samples in homogeneous fields with a Bruker DMX-300 spectrometer and compared to results obtained by the NMR MOUSE. In Fig. 8 transverse relaxation times

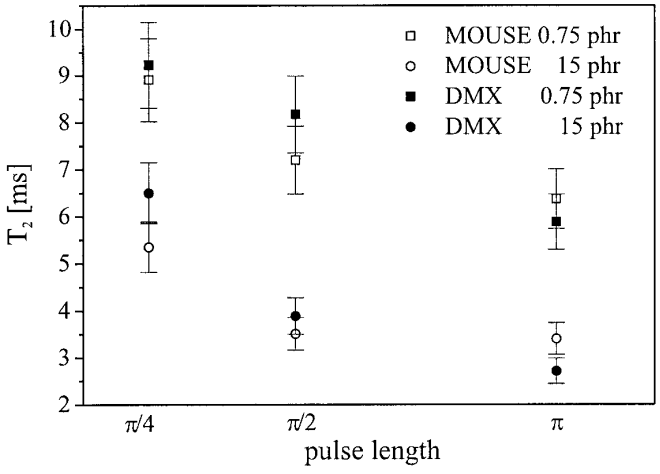

FIG. 8. Dependence of the transverse relaxation times on the flip angle for different DICUP contents (cross-link densities). Note the overall agreement between measurements by the MOUSE at 17.5 MHz and under conventional NMR conditions (DMX-300, 300 MHz). The comparison suffers from a multiexponential decay as well as magnetization modulation in the case of the MOUSE (see also Fig. 2) and from different B_0 fields for the MOUSE and the DMX-300 spectrometer.

are shown for unfilled SBR samples with different DICUP contents. The cross-link density increases with increasing DICUP content. The dependence of the effective transverse relaxation time T_2 on the flip angle and also the absolute values are comparable on both instruments. Due to the intrinsic flip angle distribution, the dependence of the transverse relaxation time T_2 on the pulse length is weaker in the case of the NMR MOUSE. However, the difference between the two samples can clearly be detected also by the NMR MOUSE, which is direct proof that mechanical properties of elastomers can be monitored by relaxation measurements with the MOUSE as already stated for conventional NMR. The reason for different relaxation times is differences in mobility of polymer chain segments. High mobility leads to efficient averaging of dipolar interactions, leaving only a residual dipolar interaction. It scales with the square of the end-to-end vector between cross-link points in a rubber network (*15*) and is the main relaxation path for protons in elastomers. Consequently the sample with higher cross-link density (15 phr DICUP) exhibits a shorter T_2 relaxation time, i.e., a higher efficiency of dipolar relaxation.

Apart from the possibility to vary the cross-link density via variation of the cross-linker content, the cross-link density changes with curing time. It first increases with increasing curing times, which implies shorter T_2 relaxation times, until it decreases as overcure sets in (*1*). Measurements on an industrial series are compatible to this reasoning. Again, results by the NMR MOUSE display the same trend as those obtained by the DMX-300 spectrometer (Fig. 9): The vulcanization process is finished after 10 min (specification by the manufacturer). The NMR data shown in Fig. 9 are in good agreement with this statement despite the fact that the volumes under examination are different. In case of the DMX-300 a volume average over a bulk sample is taken, whereas the NMR MOUSE observes only the surface regions of the sample.

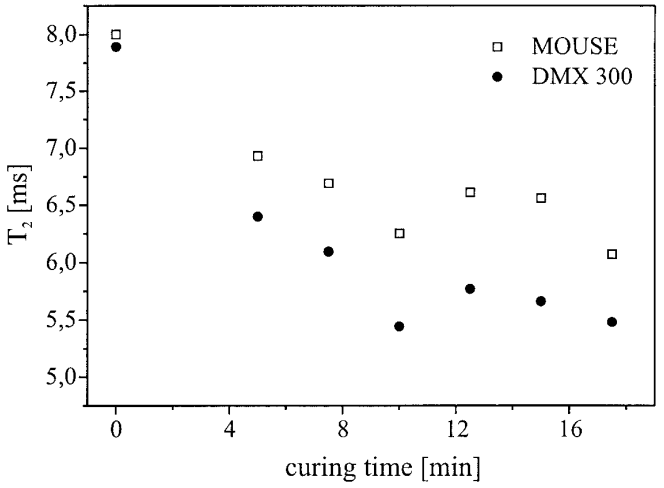

FIG. 9. Influence of the curing time of a technical rubber on the T_2 relaxation parameter. The functional dependence of both parameters is similar when observed with the MOUSE and the DMX-300. After 10 min, curing is complete, and inversion is observed beyond this point.

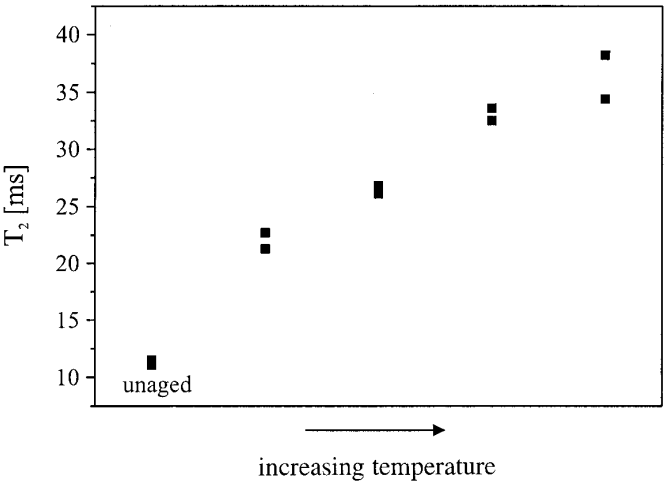

FIG. 10. Aging processes of PVDF in oil monitored by T_2. The reliability of the method was examined by measuring two independently prepared samples at each aging temperature.

Another application of the MOUSE is in monitoring the aging processes of polymers. Polyvinylidendifluorine (PVDF) samples were heated in oil at different temperatures. The associated aging process was monitored by measuring the relaxation parameter T_2 at room temperature (Fig. 10). A systematic dependence on temperature is observed. Two samples independently prepared at each temperature were measured in order to show the variance in sample homogeneity. The increase in T_2 corresponds to enhanced molecular mobility. Possible mechanisms for the increased mobility are chain scissions with increasing probability at higher temperatures and diffusion of oil into the samples. The oil could act as a plastiziser and therefore enhance the T_2 relaxation time.

In summary it is shown that the NMR MOUSE is suitable for investigations of relaxation parameters in technical samples. Properties of elastomers like cross-link density and aging of polymers can be monitored. Measurements of the same samples by conventional NMR and by the NMR MOUSE show comparable results. The signal-to-noise ratio in MOUSE measurements is enhanced by use of a modified SSFP sequence. Further investigations concerning the improvement of pulse sequences are in progress.

ACKNOWLEDGMENTS

Industrial cooperations are acknowledged to B. Hock (PIRELLI Reifenwerke GmbH, Hoechst), Dr. H. Dummler (Continental AG, Hannover), and Dr. D. Schulze (SHELL International Chemicals B.V.) for sample preparation. L. Gaspar is thanked for conducting the measurements of the curing series on the DMX-300. K. Kupferschläger solved many mechanical problems. G. Zimmer is grateful to DFG for financial support.

REFERENCES

1. P. Blümler and B. Blümich, *Rubber Chem. Technol.* (1997), and references therein.
2. C. Fülber, B. Blümich, K. Unseld, and V. Herrmann, Kautschuk Gummi Kunststoffe, **48,** 254 (1995).
3. P. Sotta, C. Fülber, D. E. Demco, B. Blümich, and W. Spiess, *Macromolecules* **29**(19), 6222 (1996); C. Fülber, D. E. Demco. O. Weintraub, and B. Blümich, *Macromol. Chem. Phys.* **197,** 581 (1996); D. Hauck, P. Blümler, and B. Blümich, *Macromol. Chem. Phys.* **198,** 2729 (1997).
4. G. Eidmann, R. Savelsberg, P. Blümler, and B. Blümich, *J. Magn. Reson. A* **122,** 104 (1996).
5. G. A. Matzkanin, *in* ''Nondestructive Characterization of Materials'' (P. Höller, V. Hauck, C. O. Rund, and R. E. Green, Eds.), Springer-Verlag, Berlin (1989).
6. D. Gill and S. Meiboom, *Rev. Sci. Instrum.* **29,** 688 (1958).
7. P. Mansfield and D. Ware, *Phys. Rev. Lett.* **22,** 133 (1966); D. Ostroff and J. S. Waugh, *Phys. Rev. Lett.* **16,** 1097 (1966).
8. R. L. Vold, R. R. Vold, and H. E. Simon, *J. Magn. Reson.* **11,** 283 (1973).
9. D. G. Hughes and G. Lindblom, *J. Magn. Reson.* **26,** 469 (1977).
10. T. Gullion, D. B. Baker, and M. S. Conradi, *J. Magn. Reson.* **89,** 479 (1990).
11. T. B. Benson and P. J. McDonald, *J. Magn. Reson. A* **112,** 17 (1995); T. B. Benson and P. J. McDonald, *J. Magn. Reson. A* **109,** 314 (1995).
12. B. J. Suh, F. Borsa, and D. R. Torgeson, *J. Magn. Reson. A* **110,** 58 (1994).
13. R. Bradford, C. Clay, and E. Strick, *Phys. Rev.* **84,** 157 (1951); H. Y. Carr, *Phys. Rev.* **112,** 1693 (1958).
14. R. R. Ernst, G. Bodenhausen, and A. Wokaun, ''Principles of Nuclear Magnetic Resonance in One and Two Dimensions,'' Clarendon Press, Oxford (1994).
15. J. P. Cohen Addad, *Prog. NMR Spectrosc.* **25,** 1 (1993).